Detecting ancient life: investigating the nature and origin of possible stromatolites and associated calcite from a one billion year old lake

A.T. Brasier, P.F. Dennis, J. Still, J. Parnell, T. Culwick, M.D. Brasier, D Wacey, S.A. Bowden, S. Crook, A.J. Boyce, D.K. Muirhead

Abstract

Putative stromatolites and associated carbonate minerals in 1.1 Ga Stoer Group lacustrine sedimentary rocks were analysed to deduce their likely origins. Potential stromatolite examples included finely laminated and sometimes wrinkled carbonate-siliciclastic rocks of the Clachtoll Formation at Clachtoll and Bay of Stoer, and laminated limestone domes of the Poll a'Mhuilt Member (Bay of Stoer Formation) from Enard Bay.

Petrography shows that the lamination and wrinkling of Clachtoll Formation specimens can most logically be explained by abiotic siliclastic sedimentary processes, namely rippling and soft-sediment deformation probably related to de-watering. Electron backscatter diffraction shows that the carbonate in these laminated Clachtoll Formation specimens was calcite, and petrography combined with clumped isotope palaeothermometry indicates it was likely to be part syn-depositional and part burial diagenetic in origin.

The laminated domes of the Poll a'Mhuilt Member are shown to comprise clasts of limestone interlayered with clay, quartz, Na-rich feldspars and micas. Cathodoluminescence revealed the limestone clasts to be composite and built of sub-grains that must have been derived from an earlier, potentially Palaeoproterozoic, carbonate unit. Support for this hypothesis comes from clumped isotope palaeotemperature measurements that indicate the limestone clasts were precipitated or recrystallized under higher temperature conditions than the burial diagenetic calcite found in the Clachtoll Formation. Raman spectra of an organic carbon particle within a laminated dome of the Poll a'Mhuilt Member at Enard Bay are consistent with the organic carbon having been re-worked from the ~ 2 Ga Loch Maree Group , and we speculate that this might also be true of the calcite.

Microbial fossils are well known from elsewhere in the Stoer Group, but no conclusive examples were found within the thin-sections examined herein. No conclusive evidence was found to suggest that any of the examined putative stromatolites were biogenic, leading to the conclusion that they are best considered stromatolite-like sedimentary rocks (pseudostromatolites).

Highlights

- **Putative stromatolites of the Mesoproterozoic Stoer Group show no evidence for biogenicity**
- **Some are laminated clastic sediment draped over an ancient land surface**
- **Clastic carbonate is calcite, probably derived from weathering of older rocks**
- **Other possible stromatolites result from soft-sediment deformation**
- **Crystalline calcite in these is a result of syn-depositional to burial diagenesis**

Key words: microbial, biogenic, clumped isotope, Mesoproterozoic, carbonate petrography, terrestrialization

Introduction

The search for fossils of ancient microscopic life usually begins with identification of a visible macro-scale target. Very commonly this is a stromatolite, defined as a laminated benthic microbial deposit (see Riding, 1999). It is now generally accepted that there is more than one way to make a layered rock, such that not all purported stromatolites are biogenic (see for example Grotzinger and Rothman, 1996; Brasier et al., 2015). Nevertheless there is growing "stromatolite"-based support for the argument that terrestrial environments around the globe were inhabited by microbial mats since the Archaean (Bolhar and van Kranendonk, 2007; Awramik and Buccheim, 2009; Fedorchuk et al., 2016; Wilmeth et al., 2019). By necessity, convincing cases for stromatolite biogenicity must usually be built on circumstantial evidence including macro- and micro-scale morphology and microtextures. Few purported early terrestrial stromatolites preserve unambiguous included microfossils.

The late Mesoproterozoic to Neoproterozoic Torridonian Supergroup sediments of Scotland, UK (Fig. 1), present an interesting case in that shale horizons contain unquestionable if allochthonous organic carbon microfossils including early terrestrial eukaryotes (Downie, 1962; Cloud and Germs, 1971; Strother et al., 2011; Wacey et al., 2014; 2017). Given the reliance on stromatolitic morphology as an indicator of ancient terrestrial life elsewhere in the Mesoproterozoic, it is useful to consider the origins of apparently stromatolitic structures in environments like those of the Stoer Group (at the base of the Torridonian Supergroup) where we know microbial life existed.

The Stoer Group is dominantly siliciclastic with few carbonate rock horizons (see Stewart, 2002; Parnell et al., 2014; Stueeken et al., 2017; Brasier et al., 2017). Notably there are layered carbonate units in the Stoer Group that have been interpreted as stromatolitic (Upfold, 1984; Krabbendam, 2011; Brasier et al., 2017), and these are the only potential macrofossils visible in the field, but their biogenicity has never been convincingly proven (Stewart, 2002). More autochthonous evidence for Stoer Group microbial life comes from "microbially induced sedimentary structures" (MISS; Noffke et al., 1996; 2001; Noffke, 2009) including desiccation cracks in cohesive sands at Rubha Reidh that are interpreted as an indication of biofilms binding the sediment (Prave, 2002). A recent study of the Meall Dearg Formation at Rubha Reidh concurred that potential MISS structures are present, including sinuous shrinkage cracks interpreted as *Manchuriophycus* (McMahon and Davies, 2017). Reduction spots with vanadium-rich micas at their centres are found in the Stoer Group rocks immediately below the Stac Fada Member and these have also been interpreted as a possible indicator of contemporaneous (Mesoproterozoic) intra-sediment microbial activity (Spinks et al. 2010).

Here we describe and critically examine some stromatolitic carbonate and siliciclastic rocks of the Stoer Group to try to ascertain their origins. Given that we know that some Stoer Group environments were inhabited by microorganisms (Strother et al., 2011) we set out to discover whether or not microorganisms were intimately associated with the "stromatolites"? Alternatively, were the latter abiogenic, and thus misleading as visible macro-scale targets in the search for ancient terrestrial life here? The aim was to investigate whether some or all of the potential terrestrial stromatolites encountered in the Stoer Group form robust autochthonous evidence for colonisation of an ancient terrestrial surface by carbonate-precipitating benthic microbial mats.

Geological context of the Stoer Group

The Late Mesoproterozoic Stoer Group in the northwest of Scotland comprises red coloured mudstones, siltstones and sandstones with a more minor carbonate component (cf. Stewart, 2002). A meteorite impact breccia within the succession known as the Stac Fada Member has been Ar-Ar age-dated to 1177±5 Ma (Amor et al., 2008; Parnell et al., 2011; Fig. 1). Archaean to Palaeoproterozoic 'Lewisian' gneisses directly underlie the Torridonian Supergroup succession and are found as clasts in the Stoer Group rocks, particularly in the Clachtoll Formation at the base of the Stoer Group stratigraphy. The eroded top of the Lewisian gneisses constituted a land surface in the Mesoproterozoic that is now exhumed and well exposed in locations including Clachtoll and Enard Bay (Figs. 1 and 2; see also Stewart, 2002; Brasier et al., 2017).

Sedimentary structures in Stoer Group rocks include normally graded beds topped by symmetrical oscillation ripples and cut by abundant sand-filled desiccation cracks. Rain drop impressions have been reported (Strother and Wellman, 2016). Chicken-wire texture formed by calcite pseudomorphing anhydrite is found in several places (Stueeken et al., 2017), and Parnell et al. (2010) and Wacey et al (2017) have noted that evaporitic and probably also bacteriogenic sulphates were a particular feature of the Stoer Group. Overall the sedimentology and stratigraphy including trough cross-bedded sandstones and unidirectional current indicators are consistent with a dominantly terrestrial fluvial and lacustrine origin (Stewart, 2002; Ielpi et al., 2016; Lebeau and Ielpi, 2017; McMahon and Davies, 2017; Brasier et al., 2017), though recently Stueeken et al. (2017) suggested on the basis of $^{87}Sr/^{86}Sr$ isotopes, $\delta^{98}Mo$ isotopes and a purported case of herringbone cross-stratification that a specific three to 30m thick section in the middle of the Poll a'Mhuilt Member of the Bay of Stoer Formation might have been deposited in marine conditions. Carbonate horizons

described as stromatolites by Upfold (1984) are within this Poll a'Mhuilt Member section at Bay of Stoer according to the grid references he provided. Upfold (1984) described possible Stoer Group stromatolites as being polygonal and stellate carbonate patches forming tuft-like growths within siliciclastic sediment, albeit affected by later compaction during burial. Stewart (2002) in consultation with Janine Bertrand-Sarfati suggested these might originally have been anhydrite nodules rather than microbial carbonate build-ups. However possible stromatolites (Riding, 1999) are not restricted to this section of the stratigraphy. Some of the best examples that form a focus of the present study are found in the Clachtoll Formation at the base of the Stoer Group including at Bay of Stoer and Clachtoll.

Methods

Petrography

Fieldwork was undertaken over several seasons from August 2009 onwards. Carbonate mineral horizons were identified in the field using 1% HCl, then subsequently described and in some cases sampled. To preserve the outcrops the majority of samples were taken as representative loose blocks or cobbles, many of which could be correlated with horizons exposed in-situ without difficulty. In the laboratory, rock specimens were cut and imaged with a zoom stereomicroscope (Nikon SMZ25) at the University of Aberdeen. These rocks were also stained with Alizarin Red S and Potassium Ferricyanide (Dickson, 1965). In Aberdeen thin-sections were examined with a petrographic microscope (Nikon Microphot FX equipped with Nikon DS Fi2 camera and Nikon Elements D software), and optical cold cathode cathodoluminescence (CL) microscope (CITL Mk 3) at 10 kV with a current of c. 350 micro amps. Representative thin-sections were also sent to the Centre for Microscopy, Characterisation and Analysis (CMCA) at the University of Western Australia where they were similarly inspected with a CarlZeiss Axioskop 2 Plus petrographic microscope. Scanning electron microscopy (SEM) was conducted in the Aberdeen Centre for Electron Microscopy, Analysis and Characterisation (ACEMAC) facility at the University of Aberdeen using a Carl Zeiss GeminiSEM 300 VP equipped with Deben Centaurus CL detector, an Oxford Instruments NanoAnalysis Xmax80 EDS detector, Oxford Instruments NordlysNano EBSD detector and AZtec software suite. In preparation for EBSD, samples were polished by hand on a glass plate using 0.3µm alumina. Prior to electron microscopy at ACEMAC the polished blocks and thin-sections were sputter coated with a thin coat of carbon under vacuum.

Raman spectroscopy

Ramon spectroscopy measurements of carbonaceous material are based on two broad Raman bands (spectral peaks) at ~1585 cm^{-1} (the graphite peak , G) and ~1350 cm^{-1} (the disorder peak, D), produced by Stokes Raman scattering, induced by a laser. Due to the physical properties of carbonaceous materials the bands are produced as a response to the ratio of sp^2 (graphite-like, trigonal planar symmetry) and sp^3 (diamond-like, tetrahedral symmetry) carbon bonds, based on the hybridised atomic orbital configuration of carbon atoms (Robertson 1991). The ca. 1585 cm^{-1} graphite peak is in fact a composite of several Raman bands at ca. 1615 cm^{-1}, ca. 1598 cm^{-1} and ca. 1545 cm^{-1} and is treated as one spectral peak in disordered materials until, through increasing thermal alteration, the band narrows sufficiently for clear definition of the shouldered disorder peaks. Increased thermal maturation leads to the structural reordering of carbonaceous materials, with an increase in the proportion of aromatic carbon, in turn narrowing the G band and shifting it closer towards 1615 cm^{-1} (see Wopenka & Pasteris, 1993). If samples are graphitic, narrowing is similar but with G peak position shifted downwards to~1598 cm^{-1}.

Raman measurements were performed on a Renishaw inVia reflex Raman spectrometer at the University of Aberdeen. A Leica DMLM reflected light microscope was used to focus the Ar^+ green laser (wavelength 514.5 nm). The laser spot size was approximately 1-2 μm and laser power between 10-50% (<13 mW power at the sample). The scattered light was dispersed and recorded by means of a CCD (Charge Coupled Device) detector. Data were collected between 1100cm^{-1} and 1700cm^{-1} with spectral resolution less than 3cm^{-1}. The duration of accumulations was typically up to 10 seconds for between 3 and 5 accumulations. Care was taken to ensure that the sample did not experience any laser-induced heating, by careful analysis under the microscope before and after interaction with the laser.

The Renishaw WiRE 2.0 curve-fit software was used for spectral deconvolution. Smoothing and baseline extractions were performed on each sample, including a cubic spline interpolation. Each sample was deconvolved and data extracted at least three times to ensure reproducibility and the removal of any background signal. Peak position and peak full width at half maximum (FWHM) are measured in wavenumbers (cm^{-1}), which records the change in vibrational frequency (stretching and breathing) of the Raman-active carbon molecules.

Stable isotope geochemistry

Rock samples were hand-drilled to produce powders for stable isotope analysis at SUERC, VU University Amsterdam, and the University of East Anglia. At SUERC, 1mg carbonate powders were dissolved in 103% phosphoric acid at 70 ºC overnight, and CO_2 produced was analysed on an AP 2003 mass spectrometer. Repeat analyses of NBS-18 and internal calcite standards are generally better than +/- 0.2 ‰ for carbon and 0.3 ‰ for oxygen. At VU University Amsterdam, carbonate samples of 50 µg weight were dissolved in individual tubes of phosphoric acid overnight at 45 ºC and analysed using a ThermoFinnigan Delta Plus with GasBench II. Repeat analyses of an internal calcite standard calibrated to NBS-19 are generally better than ±0.1‰ for carbon and ± 0.15‰ for oxygen.

Clumped isotope palaeothermometry

Measurement of carbonate Δ_{47} (dominantly $^{13}C^{18}O^{16}O$) values was undertaken at the University of East Anglia. Between 5 and 10 mg of carbonate material was hand-drilled from collected specimens and reacted with 102% (equivalent to 1.92 g/ml density) phosphoric acid offline at 25 °C prior to CO_2 clean-up on a glass vacuum line. Gases equilibrated at room temperature and at 1000 °C were measured on the UEA dual inlet MIRA (Multi-Isotopologue Ratio Analyser) mass spectrometer alongside the samples to establish a transfer function between the local and absolute reference frames (Dennis et al., 2011; see also Kirk, 2017). Internal carbonate standards (UEACMST) were also measured. Temperature calibration of carbonate Δ_{47} was done following the UEA calibration outlined in Kirk (2017) that is otherwise similar to those of Petrizzo et al. (2014) and Wacker et al. (2014).

Results

Field Descriptions

Clachtoll Formation at Clachtoll

The Clachtoll Formation at the base of the Stoer Group is well exposed in coastal sections at Clachtoll (Figs. 1 and 2). The contact with underlying Lewisian gneiss is unconformable and cobble to boulder-sized clasts of the gneiss are encapsulated within trough cross-bedded red sandstones at

the base of the section. Higher up in the Clachtoll Formation the number of large (tens of centimetre-sized) gneiss clasts decreases significantly. Here there are beds of coarse sandstones, siltstones and mudstones.

Putative stromatolite horizons within the Clachtoll Formation include thin (c. 5 to 10 cm) beds comprised of red mudstone, buff coloured carbonate and grey siliceous laminae that are mm- thick (Fig. 2). These laminated sections can be traced horizontally over distances of tens of centimetres to metres and are found between thicker (30 cm to 1m) sandstone beds with erosional bases (Fig. 2). In places the laminae are gently undulating, and otherwise the rock appears flat laminated. Millimetre-scale porosity can be seen within some of the weathered layers.

Rippled red-brown siltstones intercalated with laminae of buff coloured calcite and laminae of white mica were also encountered in the Clachtoll Formation. Plan view observations reveal sheets of these bedding-parallel carbonate and silicates are weathered out into circular patterns, giving rise to a “stromatolite-like” dome appearance in outcrop (Fig. 3A). In several cases the ripple crests, spaced two to three centimetres apart, are clearly seen to coincide with the tops of ~1cm high antiformal “stromatolite-like” structures that are best seen in cross-sections through the mud, silt and carbonate laminae (ATB 290717-5; Fig. 3B). Below several ripple crests the laminae are broken up, being much disturbed and convolute (ATB 290717-5; Fig. 3C). Below some ripple crests are apparent cracks cutting sub-vertically through the carbonate-siltstone laminae. These cracks are filled with medium to coarse sand grains sourced from underlying layers. An example of this can be seen in specimen ATB 290717-1 (Fig. 4). Some of these antiformal structures were evidently originally siliciclastic in nature, but their weathered margins are now cemented with calcite (Fig. 4). These calcite patches have sharp and clearly defined boundaries and it seems the carbonate grew diagenetically, in part spatially following the lamination on the margins of the antiformal structures.

Clachtoll Formation at Bay of Stoer

The unconformity between Lewisian Gneiss and the Torridonian sediments can be observed above the graveyard at Stoer (NC04102842; Stewart, 2002). This comprises breccia plastered against the side of Lewisian outcrop. The Clachtoll Formation is well exposed on the coast between grid references NC03832831 and NC03712835 (Stewart, 2002; Fig. 1). This begins with c. 15 cycles of sandstone, siltstone and mudstone with mudcracks. These cycles are overlain by sandstone conglomerates, and then by red-brown coloured mudstones with centimetre-thick layers of laminated and crinkled carbonate-siliciclastic couplets that might be seen as possible stromatolites. Above and below these are tabular sandstone and mudstone beds.

Clachtoll Formation - Petrography

Layered rocks from the Clachtoll Formation at Clachtoll were examined using electron microscopy (Fig. 5). EDS element maps confirm that most of the grey laminae are Na-rich aluminosilicates, with some laths of Fe-Mg silicates (micas). These silicate laminae are non-luminescent in cathodoluminescence images (black or very dark grey, Figs. 5C, 5E). The carbonate component is restricted to a few specific laminae that are recessively weathered in hand-specimen (Fig. 5A, 5B, 5D). EDS element maps confirm the carbonate phases comprise Ca – C – O (Fig. 5D, 5F), while also included in these carbonate laminae are some Fe-Mg silicates and Na-rich aluminosilicates (Fig. 5D, 5F). The remainder of the siltstone comprises re-worked (Al - Na silicate grains), quartz (Si - O), and Fe - Mg silicates. Electron backscatter diffraction showed the carbonate to be calcite, Fe-Mg silicates to be micas, and Na-rich aluminosilicates to be sodium-rich plagioclase feldspars. Cathodoluminescence images of the calcite areas reveal rather granular textures, with bright luminescent (white to light grey) euhedral to subhedral calcite crystals each measuring c. 10 µm across that are encased in a less luminescent (darker grey) calcite cement (Fig. 5E).

Poll a Mhuilt Member at Enard Bay

An undulating palaeo-land surface of eroded Lewisian Gneiss crops out at Enard Bay (Figs. 1 and 6; see also Stewart, 2009; Brasier et al., 2017). A mound of gneiss is draped in breccia that is carbonate-cemented in places. This breccia is said to include minute clasts of vitreous green tephra, presumably derived from the Stac Fada Member (Stewart, 2002), which has been taken as evidence that the carbonate cement and overlying stromatolitic limestone belong to the Poll a Mhuilt Member rather than the older Clachtoll Formation (Fig. 1). The possible stromatolites measure several tens of centimetres in width and height, draping directly over boulders of Lewisian gneiss. Internally, these possible stromatolites comprise wrinkled laminae of red siltstone that encapsulate millimetre to centimetre-sized clasts of grey-white carbonate grains (Fig. 6). Rounded clasts of gneiss measuring up to several millimetres across may also be found within the siltstone matrix (Fig. 6).

Poll a Mhuilt Member at Enard Bay - Petrography

Stereomicroscope images of cut hand-specimens reveal that the possible stromatolites of Enard Bay are comprised of carbonate mineral clasts hosted in matrices of red-brown silt (Fig. 7). Millimetre to

centimetre sized inclusions of Lewisian gneiss are prominent within the stromatolite-like textures. Many of the carbonate clasts have a preferred orientation, with long axes parallel to the specimen lamination. Several of the elongate clasts are fractured and silt matrix has infilled the cracks. The carbonate component stains purple-red with Alizarin Red S and Potassium Ferricyanide, consistent with their being calcite of a slightly ferroan composition (Dickson, 1965).

Thin-section light microscopy reveals angular clasts of quartz and feldspar in the silt component (Fig. 7). Dark micrite forms ghosts of former crystal rims in the carbonate clasts. Patches of transparent coarse spar are found interspersed with cloudy micrite. In places the edges of the calcite clasts appear resorbed as if partially dissolved prior to (or contemporaneous with) their deposition.

Cold cathode CL microscopy uncovers three different types of calcite in the potential stromatolite (Fig. 8). The first type forms the bulk of the carbonate component, comprising dull red-orange luminescent micrite. Less common are patches of non-luminescent spar within the micrite clasts. The most luminescent phase is a brighter orange. This is found in veinlets and fringing cements, cutting through both the dull luminescent micrite and the non-luminescent spar.

Cathodoluminescence (CL) under the scanning electron microscope was further informative (Fig. 9). Clasts of calcite observed by light microscopy and measuring hundreds of microns to millimetres in diameter were found under CL to be composite grains, the constituent sub-grains each 10 to 20 µm in diameter. Many of these sub-grains were rounded to angular in shape. In places these sub-grains resembled interlocking crystals rather than transported sedimentary clasts. Veins of apparently less luminescent calcite were also seen by SEM CL. These were cutting through the larger carbonate clasts and surrounding matrix.

EDS elemental maps combined with electron backscatter diffraction analyses revealed calcite clasts (artificially coloured dark blue in Fig 9) that entomb clasts of quartz (coloured green on Fig. 9) and silicates rich in sodium and aluminium (feldspars, light blue on Fig. 9). Alignment of clasts of similar sizes parallel to the carbonate clast edges (and hence parallel to the overall specimen lamination) is evident in Fig. 9. The quartz and silicate grains were also found in great abundance between the carbonate clasts where they were also associated with a matrix of aluminosilicates rich in iron and magnesium (interpreted as clays, coloured pink on Fig. 9). Potassium-rich silicates were also associated with the silt component between the carbonate clasts (yellow on Fig. 9). Close comparison of EDS and CL data reveals the non-luminescent patches between grains on Fig. 9 to be Mg and Fe-rich aluminosilicate clays.

Despite extensive searching, no filamentous or coccoid microfossils were observed in any of the thin-sections or cut blocks examined.

Isotope Geochemistry

Carbon and oxygen stable isotope compositions of Stoer Group carbonate minerals tend to plot in very restricted compositional ranges (Table 1; Fig. 10). For carbonate from the Poll a'Mhuilt Member at Enard Bay, $\delta^{18}O$ is typically -16 to -18 ‰ (VPDB) and $\delta^{13}C$ just above 0 ‰ (VPDB). Other Stoer Group carbonates examined yield $\delta^{13}C$ values between -2.8 and +1 ‰, with $\delta^{18}O$ no more negative than the -16 to 18 ‰ range as found in the Poll a'Mhuilt Member at Enard Bay, while several carbonate cements at Stoer Bay yielded slightly higher $\delta^{18}O$ values of up to -9.8 ‰ (Table 1).

Sample name	**$\delta^{18}O$ (VPDB)**	**$\delta^{13}C$ (VPDB)**	**Location**
Torr carb 5	-14.06	0.79	Stoer, Cave
Torr carb 9	-15.13	0.58	Stoer, Cave
Torrcarb 15	-11.98	-2.78	Bay of Stoer cave
Torrcarb 16	-11.34	-2.23	Bay of Stoer cave
Torrcarb 20	-14.30	-0.57	Bay of Stoer pseudomorph in black shale
Stoer-thick	-12.39	-0.06	Bay of Stoer cement in red silts
MDBStoerCalcrete	-9.78	1.63	Bay of Stoer cement in red silts
EnardBayB2	-16.35	0.45	Enard Bay stromatolite calcite
EnardBayB3	-16.23	0.87	Enard Bay stromatolite calcite
EnardBay4	-17.10	0.59	Enard Bay stromatolite calcite

Table 1: Carbonate stable isotope (O and C) values for Stoer Group carbonates

Enard Bay Poll a'Mhuilt Member carbonate clumped isotopes (Δ_{47}) yield calculated temperatures of up to c. 160 °C (following the carbonate Δ_{47} temperature calibration of Kirk, 2017). Samples of Stoer Group carbonate taken from Bay of Stoer yield clumped isotope temperatures that are lower, from a low of 60 °C up towards c. 110 °C. These calculated temperatures must be considered notional in the sense that they probably record a partial approach to clumped isotope equilibrium. Nevertheless, using these clumped isotope temperatures and the associated calcite $\delta^{18}O$ values it is possible to calculate equilibrium $\delta^{18}O$ compositions for the parent fluids. These calculated fluid compositions are also given on Fig. 11.

Raman spectroscopy

One carbonaceous inclusion was found in a thin-section of a potential stromatolite from the Poll a'Mhuilt Member, Enard Bay. Raman data for this are shown graphically in Fig. 12. This inclusion exhibits a pronounced G band around 1585 cm^{-1} and is evidently graphitic (cf Muirhead et al., 2017).

Discussion

Using a combination of field observations, petrography and geochemistry it is possible to establish the origins of two different types of domed, layered rocks that might be termed "stromatolites" sensu Semikhatov et al. (1979) or "possible stromatolites" sensu Riding (1999) in the Stoer Group. These origins are laminae deformed by sand injection (type 1), and layered clastic sediment drapes over boulders (type 2).

Type 1: lamina deformation by sand injection

Coincidence of ripple crests with antiformal structures in underlying carbonate and silt laminae can be explained by preferential compression of unconsolidated sediments below the ripple troughs (Figs. 3 and 4). This pressure could have come from loading due to accumulation of sediment in the ripple troughs, pushing down in the troughs and thereby forcing the underlying laminae to flex upward beneath ripple crests. Support for this hypothesis comes from the disrupted and convolute lamination below the ripple crests that was probably caused by fluid movement: a common phenomenon in Torridonian environments that lacked vascular vegetation (Owen, 1995; Owen and Santos, 2014). The fact that carbonate laminae were broken and disrupted prior to lithification of the sediment indicates that at least here the primary mineral (calcite or its precursor, e.g. potentially gypsum in some cases) was syn-sedimentary in origin. It is also notable that in several cases the antiformal shapes are formed by carbonate-free siliciclastic laminae, transitioning laterally in places to calcite cemented laminae (Fig. 4). In most or all these cases the siliciclastic lamination is the result of grain size differences (silt to sand) and easily explained by abiotic aqueous sedimentary processes, potentially related to temporal variations in fluvial discharge to the lake. It seems evident that much of the calcite was secondary, and grew within siliciclastic layers and thereby not in the presence of light.

It is hard to tell whether some of the calcite in the Clachtoll Formation laminated sections (e.g. Fig. 5) was re-worked grains or autochthonous crystals that have been cemented. When seen under

cathodoluminescence their shapes approach euhedral (Fig. 5E), but there was porosity between the calcite crystals, and feldspar and mica grains in the same layers were clearly re-worked clasts (Fig. 5E). As such, an interpretation that the calcite in these layers originated as calcite precipitated within the sediment that was subsequently transported as grains a short distance (metres or hundreds of metres) seems possible but speculative. An early burial origin is also possible for much of the diagenetic calcite if interpreting on the basis of the petrography alone.

To summarise, in several possible stromatolite cases the lamination proves to be a primary clastic lamination that was disrupted through syn-sedimentary fluid movement. The calcite in many of these specimens is a diagenetic precipitate, potentially in part syn-depositional though quite plausibly formed during burial, and is not evidently of any clear biogenic origin.

Type 2: drapes of layered sediment over boulders

The dome-shaped outward appearance of the Enard Bay stromatolites seems to be related to the draping of unconsolidated clastic laminae over rounded boulders of Lewisian gneiss (Fig. 6). The sediment itself comprises silts with clasts of quartz and feldspar that are interlayered with carbonate layers that are dominantly composed of composite calcite clasts comprised of rounded sub-grains (Fig. 9). The latter requires some transport of and re-working of the calcite prior to its inclusion in the possible stromatolite, and some grains of quartz and feldspar included in the calcite horizons further supports this assertion. Some later authigenic calcite cement growth, however, is indicated by the interlocking crystal texture visible in cathodoluminescence (Fig. 9). There does not seem to be any robust reason to consider these possible stromatolites to be true biogenic stromatolites.

Biogenicity?

Lack of entombed microbial filaments or coccoids does not definitively rule out a microbial role in some of the authigenic calcite precipitation, but without further evidence any suggestion that the carbonate (or a component of it) was biologically-mediated is at best speculative.

The only organic carbon found and analysed by Raman spectroscopy was a graphitic inclusion in a thin-section of a possible stromatolite from the Poll a'Mhuilt member at Enard Bay (Fig. 12). The Raman Shift and Scattering Intensity of this sample are very similar to those obtained from Palaeoproterozoic graphite of the Loch Maree Group and dissimilar from kerogen previously reported from the Stoer Group (Muirhead et al., 2017 and Fig. 12). A cross-plot of Full Width Half

Maximum of the G-band peak (cm^{-1}) versus G band position (cm^{-1}) further demonstrates the similarity between the Poll a'Mhuilt graphitic inclusion and Loch Maree Group graphite (Fig. 13). A simple explanation for this is that the graphite in the Poll a'Mhuilt specimen is not actually Neoproterozoic but is re-worked organic carbon from the older Palaeoproterozoic (~2.0 Ga) Lewisian Loch Maree Group rocks. It is therefore also possible that some of the calcite was derived from rocks of the Loch Maree Group (c.f. Kerrysdale Belt carbonates of Kerr et al., 2016).

Isotopes and origins of Stoer Group calcite

The range of carbonate $\delta^{18}O$ and $\delta^{13}C$ values is similar to findings of previous authors including Parnell et al. (2014), who found Stoer Group calcites exhibited $\delta^{13}C$ from -2.0 to +0.8 ‰ VDPB, and $\delta^{18}O$ from -15.1 to -10.9 ‰ VDPB. Unfortunately the measured carbon isotope values do not help with diagnosis of any particular depositional process or carbonate source so they are not considered further here.

The reported carbonate clumped isotope temperatures are somewhat more illuminating regarding the calcite origins. Temperatures calculated for specimens except the possible stromatolites of the Poll a'Mhuilt Member of Enard Bay (i.e., except those with clearly allochthonous granular re-worked calcite) are reasonably similar in range to those measured from fluid inclusions of distinctive bedding-parallel calcite veins in the Stoer Group (74 to 80 °C, with an outlier at 140 °C; Parnell et al., 2014). Parnell et al (2014) attributed these high-temperature calcite veins to a Mesoproterozoic burial diagenetic origin. Given the similar geochemistry, it seems likely that much of the diagenetic calcite described in the present study was either formed or recrystallized under similar Mesoproterozoic burial conditions. Recalling that cross-cutting relationships are consistent with at least some of this diagenetic calcite being syn-depositional an interpretation of a widespread re-setting of carbonate clumped isotope temperatures during burial in the Mesoproterozoic seems likely.

396 It is alternatively conceivable that the c. 80 °C clumped isotope temperatures might have been
397 recorded during prograde metamorphism of Lewisian rocks during the Neoproterozoic Knoydartian
398 orogeny (Tanner and Evans, 2003). If fluid: rock ratios were very low then it is possible that the
399 clumped isotope temperatures could have been re-set via grain boundary migration during
400 thermally induced grain growth (cf. Covey-Crump and Rutter, 1989), but that the carbonate $\delta^{18}O$
401 values were rock buffered so remained rather invariant. Thermally induced grain growth seems
402 more likely to proceed as temperatures increase under prograde metamorphism. Counter to this,
403 Parnell et al. (2014) noted that veins attributed to metamorphism in the Stoer Group are dominantly
404 made of quartz and pumpellyite rather than calcite (Hay et al., 1988; Stewart, 2002), so perhaps
405 unlikely to be the result of prograde metamorphism.

406

407 In either case (burial diagenesis or low-grade metamorphism) the c. -17 ‰ $\delta^{18}O$ carbonate values
408 might be interpreted as derived from equilibration with a fluid $\delta^{18}O$ close to +4 ‰ VSMOW at 160 °C
409 (following, for example, relationships given in O'Neil et al., 1969), perhaps with some variable
410 resetting during cooling if a retrograde process. If so, then the pattern of variable clumped isotope-
411 derived temperatures at near constant carbonate $\delta^{18}O$ values must represent partial resetting during
412 cooling under very low water to rock ratios. These isotope geochemical interpretations all obviously
413 assume that the calcite precipitated in isotopic equilibrium with its parent fluid.

414 Returning to the samples from the Poll a'Mhuilt Member at Enard Bay, petrography shows that
415 these clearly contain re-worked calcite grains (Figs. 7 and 9), so it seems logical that the generally
416 higher temperatures measured (up to 160 °C) could have been imparted during an earlier phase of
417 burial or metamorphism. This source could have been the Palaeoproterozoic Loch Maree Group,
418 given the likely source of included organic carbon. It is arguable on the basis of the carbonate
419 clumped isotopes (Fig. 11), coupled with the Raman spectra of associated organic matter (Fig. 13),
420 that the calcite that forms many of the laminae in the possible stromatolites of the Poll a'Mhuilt

Member at Enard Bay was not actually precipitated in the Stoer Lake. Rather, this clastic sediment was derived from erosion and re-working of underlying Palaeoproterozoic rock. No clear evidence for any biologically-influenced calcite was found in association with the possible Stoer Group stromatolites studied.

If the clastic limestone in the Poll a'Mhuilt Member at Enard Bay was derived from erosion and re-working of Palaeoproterozoic Lewisian carbonate rocks then this raises questions on the origin of the carbonate in the Poll a'Mhuilt Member at Bay of Stoer from which purported marine geochemical signals have been obtained (Stueeken et al., 2017). Further petrographic and geochemical investigation of the carbonate in that section may be warranted to verify its assumed autochthonous nature.

Wider implications

A clear outcome of this study was the lack of any unambiguous microfossils in the purported stromatolites. This is far from unusual, and others have found microfossils to be absent in purported stromatolites of, for example, the terrestrial Mesoproterozoic Copper Harbor Conglomerate (Michigan, USA; Wilmeth et al., 2014; Fedorchuk et al., 2016). However the fact that organic carbon microfossils have been recovered by others from shales of the Stoer Group (Downie, 1962; Cloud and Germs, 1971; Strother et al., 2011; Wacey et al., 2014; 2017) leads us to question whether domed and layered 'stromatolitic' sediments are forming a distraction in the hunt for ancient terrestrial microbial life. Sediment draped over boulders to form domes may be no more likely to contain fossil microbes than flat-lying lake-deposited muds that might be comparatively under-explored.

444 The observation that many of the Stoer Group pseduostromatolitic structures demonstrably relate
445 to fluid movements and soft-sediment deformation is intriguing. Many Proterozoic terrestrial
446 environments will have been at least periodically saturated with water: a situation that only changed
447 on the arrival of vascular plants in the Silurian to Devonian (Davies and Gibling, 2010; Owen and
448 Santos, 2014). We can expect that Stoer Group-like pseudostromatolitic soft sediment deformation
449 structures associated with de-watering are likely to be more abundant in Palaeoproterozoic to lower
450 Palaeozoic successions than has been reported to date.

451 **Conclusion**

452 Close examination of the petrography of potential stromatolites from the Clachtoll Formation and
453 Poll a' Mhuillt Member indicates that their geometries can all be explained by abiotic clastic
454 sedimentary processes. Soft sediment deformation is a noted feature of the Stoer Group rocks,
455 probably in part reflecting lack of vascular vegetation in a terrestrial environment, and can explain
456 many of the parallel laminated or domal shapes seen in outcrop.

457 The carbonate examined seems to be part diagenetic cement, and part reworked clastic carbonate
458 that might be from a Palaeoproterozoic source such as the ~2.0 Ga Loch Maree Group. Included
459 organic carbon is rare in the examined specimens and the only example definitively encountered
460 seems to have been derived from the Palaeoproterozoic Loch Maree Group. No unambiguous
461 microfossils were found in any of the examined specimens.

462 Carbonate clumped isotope values, coupled with carbonate oxygen isotope values, indicate high
463 calcite precipitation temperatures of up to c. 160 °C from fluids with δ^{18}Ovsmow around +4 per mil.
464 This is consistent with recrystallization of calcite during metamorphism, perhaps in part during the
465 Lewisian (included re-worked clasts) and in part during the Neoproterozoic Knoydartian orogeny
466 (much of the syn-depositional Stoer Group calcite).

In short, no unambiguously microbial stromatolites (i.e. stromatolites sensu Riding, 1999) are known from Scotland's Torridonian rocks. Rather, the "possible stromatolite" specimens examined here are better termed "probably not stromatolites".

Acknowledgements

ATB acknowledges the hospitality of the North West Highlands Geopark in July 2017. DW acknowledges funding from the Australian Research Council via the Future Fellowship scheme (FT 140100321).

References

1. Amor, K., Hesselbo, S.P., Porcelli, D., Thackrey, S., Parnell, J., 2008. A Precambrian proximal ejecta blanket from Scotland. Geology 36 (4), 303-306.
2. Awramik, S.M., Buchheim, H.P., 2009. A giant, Late Archean lake system: The Meentheena Member (Tumbiana Formation; Fortescue Group), Western Australia. Precambrian Research 174 (3-4), 215-240.
3. Bolhar, R., Van Kranendonk, M.J., 2007. A non-marine depositional setting for the northern Fortescue Group, Pilbara Craton, inferred from trace element geochemistry of stromatolitic carbonates. Precambrian Research 155 (3-4), 229-250.
4. Brasier, A., Culwick, T., Battison, L., Callow, R., Brasier, M., 2017. Evaluating evidence from the Torridonian Supergroup (Scotland, UK) for eukaryotic life on land in the Proterozoic. Geological Society, London, Special Publications 448, SP448. 13.
5. Brasier, A., Rogerson, M., Mercedes-Martin, R., Vonhof, H., Reijmer, J., 2015. A Test of the Biogenicity Criteria Established for Microfossils and Stromatolites on Quaternary Tufa and Speleothem Materials Formed in the "Twilight Zone" at Caerwys, UK. Astrobiology 15 (10), 883-900.
6. British Geological Survey, 2002, Point of Stoer. Scotland Sheet 107W, Solid and Drift Geology,1:50,000 (Keyworth, Nottingham: BritishGeologicalSurvey).
7. Burne, R.V., Moore, L.S., 1987. Microbialites: organosedimentary deposits of benthic microbial communities. Palaios, 241-254.
8. Cloud, P., Germs, A., 1971. New Pre-Paleozoic Nannofossils from Stoer Formation (Torridonian), Northwest Scotland. Geological Society of America Bulletin 82 (12), 3469-3474.
9. Covey-Crump, S.J., Rutter, E.H. 1989. Thermally-induced grain growth of calcite marbles on Naxos Island, Greece. Contributions to Mineralogy and Petrology 101 (1), 69-86.
10. Davies, N.S., Gibling, M.R., 2010. Cambrian to Devonian evolution of alluvial systems: The sedimentological impact of the earliest land plants. Earth-Science Reviews 98 (3-4), 171-200.
11. Dennis, K.J., Affek, H.P., Passey, B.H., Schrag, D.P., Eiler, J.M., 2011. Defining an absolute reference frame for 'clumped' isotope studies of CO2. Geochim. Cosmochim. Acta 75 (22), 7117-7131.
12. Dickson, J., 1965. A modified staining technique for carbonates in thin section.
13. Downie, C., 1962. So-called spores from the Torridonian. 1600, 127-128.
14. Fedorchuk, N.D., Dornbos, S.Q., Corsetti, F.A., Isbell, J.L., Petryshyn, V.A., Bowles, J.A., Wilmeth, D.T., 2016. Early non-marine life: evaluating the biogenicity of Mesoproterozoic fluvial-lacustrine stromatolites. Precambrian Res. 275, 105-118.
15. Grotzinger, J.P., Rothman, D.H., 1996. An abiotic model for stromatolite morphogenesis. Nature 383 (6599), 423.
16. Hay, S.J., Hall, J., Simmons, G., Russell, M.J., 1988. Sealed microcracks in the Lewisian of NW Scotland: a record of 2 billion years of fluid circulation. J. Geol. Soc. 145, 819e830.

17. Ielpi, A., Ventra, D., Ghinassi, M., 2016. Deeply channelled Precambrian rivers: Remote sensing and outcrop evidence from the 1.2 Ga Stoer Group of NW Scotland. Precambrian Res. 281, 291-311.
18. Kerr, G.B., Prave, A.R., Martin, A.P., Fallick, A.E., Brasier, A.T., Park, R.G., 2015. The Palaeoproterozoic global carbon cycle: insights from the Loch Maree Group, NW Scotland. Journal of the Geological Society , 2014-2042.
19. Kirk, R., 2017. Development of clumped isotope techniques and their application to palaeoclimate studies .
20. Krabbendam, M., 2011. Excursion 4: Stoer Group at Enard Bay. In: Kathryn M. Goodenough, Maarten Krabbendam (Ed.), A Geological Excursion Guide to the North-West Highlands of Scotland. Edinburgh Geological Society, Edinburgh, UK
21. Lebeau, L.E., Ielpi, A., 2017. Fluvial channel-belts, floodbasins, and aeolian ergs in the Precambrian Meall Dearg Formation (Torridonian of Scotland): Inferring climate regimes from pre-vegetation clastic rock records. Sediment. Geol. 357, 53-71.
22. O'Neil, J.R., Clayton, R.N., Mayeda, T.K. Oxygen isotope fractionation in divalent metal carbonates. The Journal of Chemical Physics 51, 5547, https://doi.org/10.1063/1.1671982
23. Muirhead, D.K., Parnell, J., Spinks, S., Bowden, S.A., 2017. Characterisation of Organic Matter in the Torridonian Using Raman Spectroscopy. In: Brasier, A.T., McLoughlin, N. and McIlroy, D. (Eds.), Earth System Evolution and Early Life: A Celebration of the Work of Martin Brasier. Geological Society of London.
24. Noffke, N., 2009. The criteria for the biogeneicity of microbially induced sedimentary structures (MISS) in Archean and younger, sandy deposits. Earth-Sci Rev 96 (3), 173-180.
25. Noffke, N., Gerdes, G., Klenke, T., Krumbein, W.E., 2001. Microbially induced sedimentary structures: a new category within the classification of primary sedimentary structures. Journal of Sedimentary Research 71 (5), 649-656.
26. Noffke, N., Gerdes, G., Klenke, T., Krumbein, W.E., 1996. Microbially induced sedimentary structures - examples from modern sediments of siliciclastic tidal flats. Zentralblatt fur Geologie und Palaontologie Teil 1 , 307-316.
27. Owen, G., 1995. Soft-sediment deformation in upper Proterozoic Torridonian sandstones (Applecross Formation) at Torridon, northwest Scotland. Journal of Sedimentary Research 65 (3).
28. Owen, G., Santos, M.G., 2014. Soft-sediment deformation in a pre-vegetation river system: the Neoproterozoic Torridonian of NW Scotland. Proceedings of the Geologists' Association 125 (5), 511-523.
29. Parnell, J., Blamey, N.J., Costanzo, A., Feely, M., Boyce, A.J., 2014. Preservation of Mesoproterozoic age deep burial fluid signatures, NW Scotland. Mar. Pet. Geol. 55, 275-281.
30. Parnell, J., Boyce, A.J., Mark, D., Bowden, S., Spinks, S., 2010. Early oxygenation of the terrestrial environment during the Mesoproterozoic. Nature 468 (7321), 290-293.
31. Parnell, J., Mark, D., Fallick, A.E., Boyce, A., Thackrey, S., 2011. The age of the Mesoproterozoic Stoer Group sedimentary and impact deposits, NW Scotland. Journal of the Geological Society 168 (2), 349-358.
32. Peach, B.N., Horne, J., Gunn, W., Clough, C.T., Teall, J.J.H., Hinxman, L.W., 1907. The Geological Structure of the North-West Highlands of Scotland. HM Stationery Office.
33. Petrizzo, D.A., Young, E.D., Runnegar, B.N., 2014. Implications of high-precision measurements of 13C–18O bond ordering in CO2 for thermometry in modern bivalved mollusc shells. Geochim. Cosmochim. Acta 142, 400-410.
34. Prave, A.R., 2002. Life on land in the Proterozoic: Evidence from the Torridonian rocks of northwest Scotland. Geology 40, 811-814.
35. Riding, R., 1999. The term stromatolite: towards an essential definition. Lethaia 32 (4), 321-330.
36. Semikhatov, M., Gebelein, C., Cloud, P., Awramik, S., Benmore, W., 1979. Stromatolite morphogenesis—progress and problems. Canadian Journal of Earth Sciences 16 (5), 992-1015.
37. Spinks, S.C., Parnell, J., Bowden, S.A., 2010. Reduction spots in the Mesoproterozoic age: implications for life in the early terrestrial record. International Journal of Astrobiology 9 (4), 209-216.
38. Stewart, A., 2009. Torridonian Rocks of Great Britain. In: Mendum, J., Barber, A., Butler, R., Flinn, D., Goodenough, K., Krabbendam, M., Park, R. and Stewart, A. (Eds.), Lewisian, Torridonian and Moine Rocks of Scotland. Joint Nature Conservation Committee.
39. Stewart, A.D., 2002. The Later Proterozoic Torridonian Rocks of Scotland: Their Sedimentology, Geochemistry and Origin.

40. Strother, P.K., Wellman, C.H., 2016. Palaeoecology of a billion-year-old non-marine cyanobacterium from the Torridon Group and Nonesuch Formation. Palaeontology 59 (1), 89-108.
41. Strother, P.K., Battison, L., Brasier, M.D., Wellman, C.H., 2011. Earth's earliest non-marine eukaryotes. Nature 473 (7348), 505-509.
42. Stueeken, E.E., Bellefroid, E., Prave, A.R., Asael, D., Planavsky, N., Lyons, T., 2017. Not so non-marine? Revisiting the Stoer Group and the Mesoproterozoic biosphere. Geochemical Perspectives Letters .
43. Tanner, P., Evans, J., 2003. Late Precambrian U–Pb titanite age for peak regional metamorphism and deformation (Knoydartian orogeny) in the western Moine, Scotland. Journal of the Geological Society 160 (4), 555-564.
44. Upfold, R.L., 1984. Tufted microbial (cyanobacterial) mats from the Proterozoic Stoer Group, Scotland. Geological Magazine 121 (04), 351-355.
45. Wacey, D., Brasier, M., Parnell, J., Culwick, T., Bowden, S., Spinks, S., Boyce, A.J., Davidheiser-Kroll, B., Jeon, H., Saunders, M., 2017. Contrasting microfossil preservation and lake chemistries within the 1200–1000 Ma Torridonian Supergroup of NW Scotland. Geological Society, London, Special Publications 448, SP448. 6.
46. Wacey, D., Saunders, M., Roberts, M., Menon, S., Green, L., Kong, C., Culwick, T., Strother, P., Brasier, M.D., 2014. Enhanced cellular preservation by clay minerals in 1 billion-year-old lakes. Scientific reports 4.
47. Wacker, U., Fiebig, J., Tödter, J., Schöne, B.R., Bahr, A., Friedrich, O., Tütken, T., Gischler, E., Joachimski, M.M., 2014. Empirical calibration of the clumped isotope paleothermometer using calcites of various origins. Geochim. Cosmochim. Acta 141, 127-144.
48. Wilmeth, D., Corsetti, F., Beukes, N., Awramik, S., Petryshyn, V., Spear, J., Celestian, A., 2019. Neoarchean (2.7 Ga) lacustrine stromatolite deposits in the Hartbeesfontein Basin, Ventersdorp Supergroup, South Africa: Implications for oxygen oases. Precambrian Res. 320, 291-302.
49. Wilmeth, D.T., Dornbos, S.Q., Isbell, J.L., Czaja, A.D., 2014. Putative domal microbial structures in fluvial siliciclastic facies of the M esoproterozoic (1.09 G a) C opper H arbor C onglomerate, U pper P eninsula of M ichigan, USA. Geobiology 12 (1), 99-108.

Figure captions

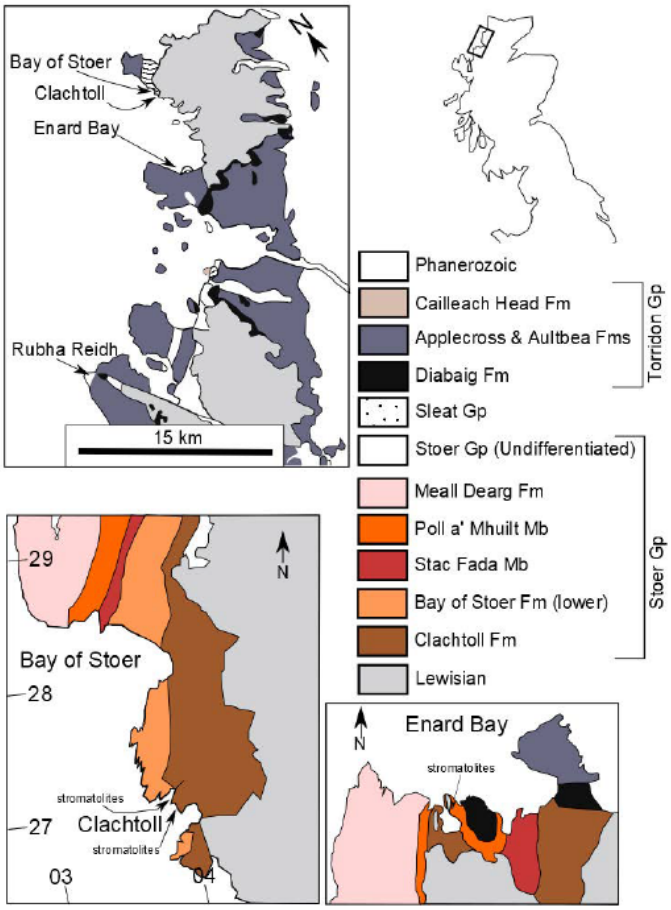

614

615 Fig. 1: Map of Stoer Group localities in northwest Scotland. Top right: map of the northern UK
616 showing the study area (black rectangle). Top left: geological map of the northwest highlands
617 modified from Stewart (2002). Bay of Stoer, Clachtoll, Enard Bay and Rubha Reidh are arrowed.
618 Lower left: geological map of Bay of Stoer and Clachtoll, modified from British Geological Survey
619 (2002). Locations of putative stromatolites are arrowed. Lower right: geological map of Enard Bay,
620 showing the location of the putative stromatolites (arrowed).

621

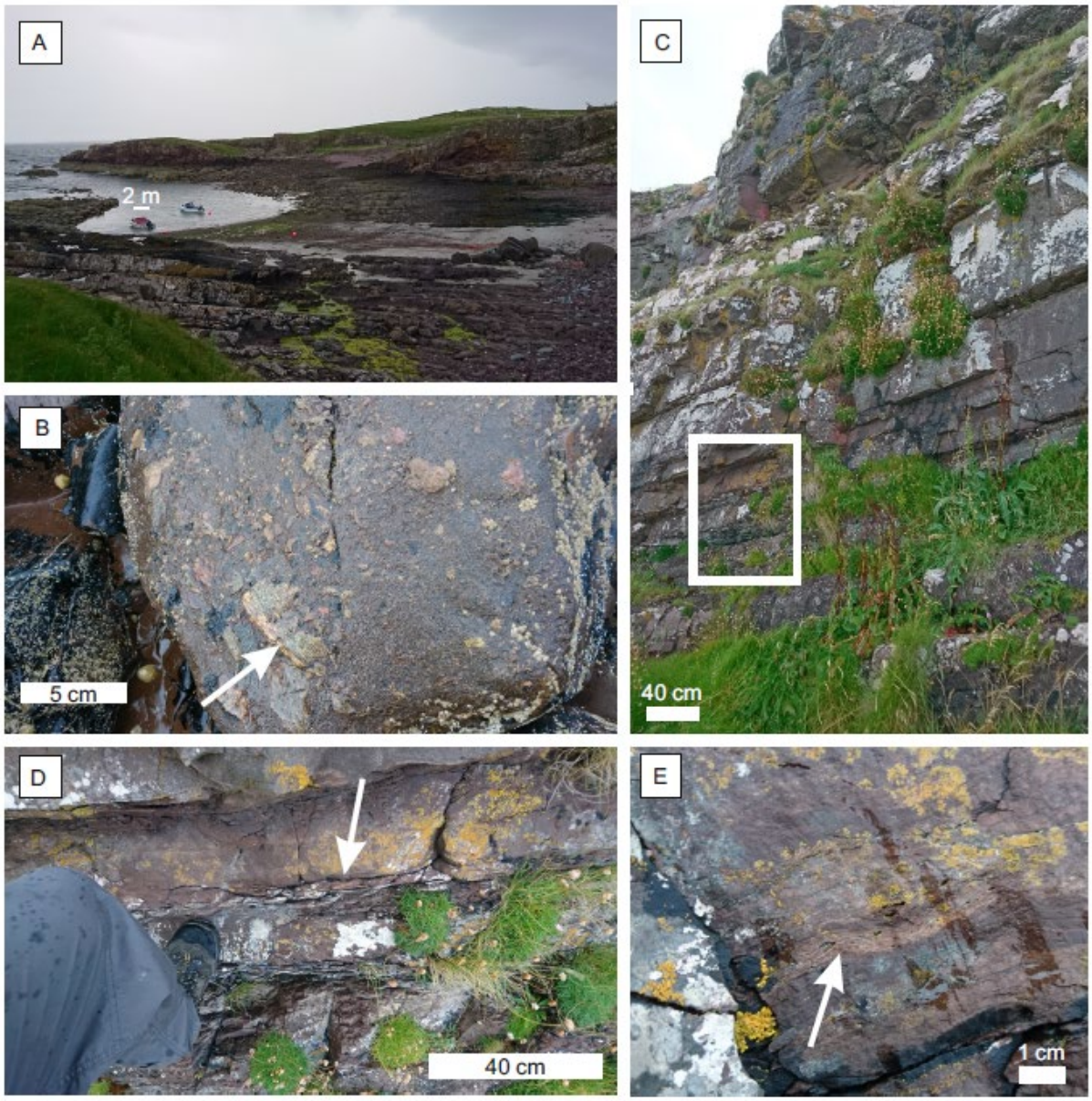

622

623 Fig. 2: Field images of Clachtoll Formation rocks as seen at Clachtoll. A) View of the bay, showing
624 rocks cropping out. B) Clasts of Palaeoproterozoic Lewisian Gneiss in conglomerates from near the
625 base of the Clachtoll Formation. C) Cliff section on the north side of the bay. White box is the area
626 shown in D. D) Red-brown mudstones and sandstones, with white arrow pointing to a horizon of
627 crinkled carbonate-siliciclastic lamination of the type that appears possibly stromatolitic in outcrop.
628 E) A close-up of such wrinkled lamination (arrowed) from the same level as shown in D.

629

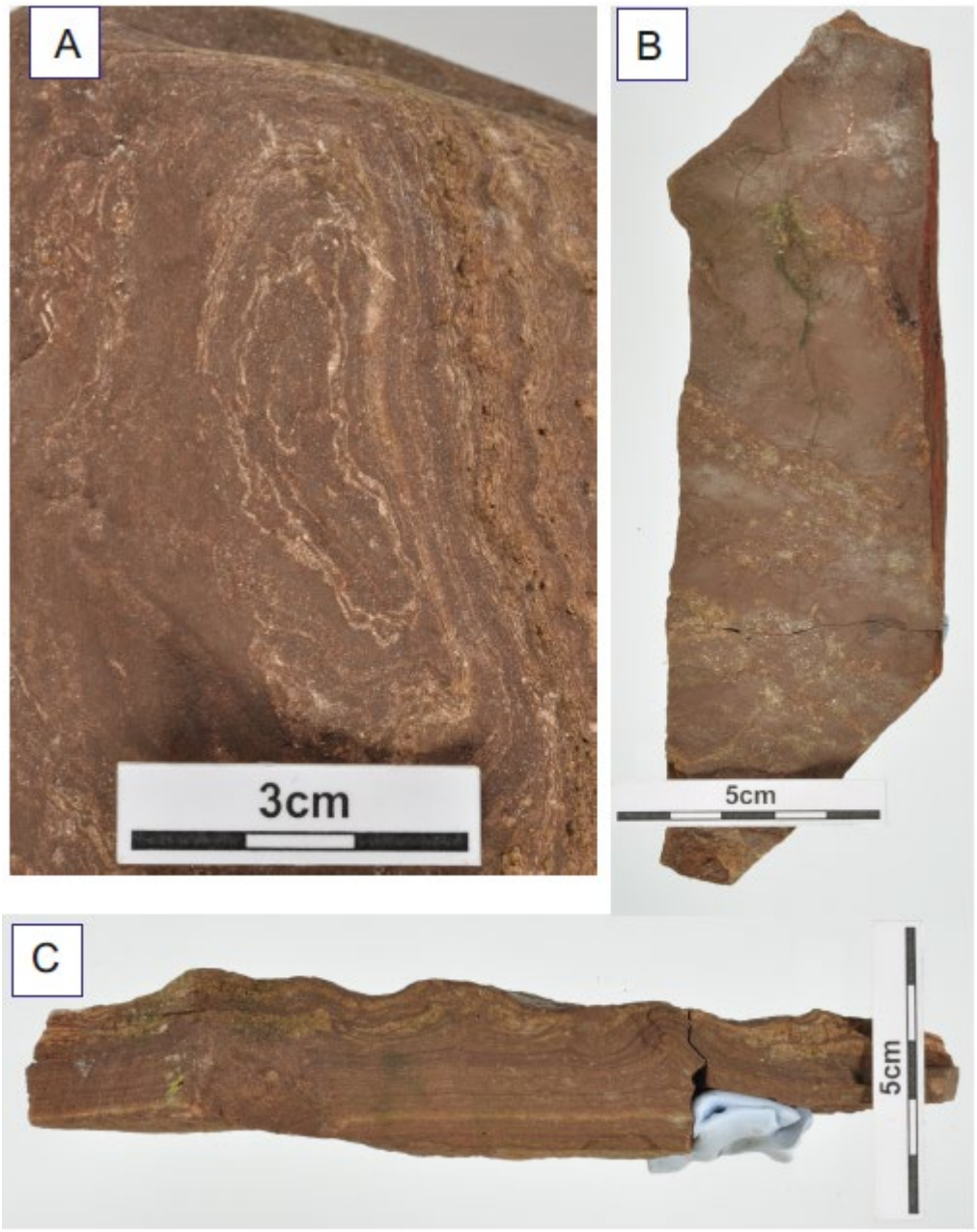

630

631 Fig. 3: Laminated siliciclastic sediments from Clachtoll Formation at Clachtoll. A, plan view of a
632 specimen eroded into a dome shape, making lighter coloured sandy and calcitic sub-horizontal
633 laminae appear as concentric rings. Such patterns are common in the Clachtoll Formation . B, plan
634 view image of a rippled sandstone from Clachtoll. Ripple crests run left to right and include coarser
635 sand within them. C, cross-section through the specimen shown in B. On the left hand side a patch of
636 coarse grained sand has risen from below to disrupt laminae, emerging at the ripple crest. Note that
637 an otherwise continuous light-coloured calcite-cemented band near the base of the specimen was
638 cut through by the injection of coarse sand.

639

Fig. 4. Cross-section through a polished specimen exhibiting domed and wrinkled lamination from the Clachtoll Formation at Clachtoll. A shows the whole specimen, and B is a close-up of the same specimen. On the left and right are white-coloured patches of diagenetic calcite cement. The remainder of the specimen lacks carbonate. The lamination is composed of red to grey coloured millimetre-thick layers of sand and silt. Coarse sand evidently rose up from the base of the specimen towards a peak in the wrinkled lamination, suggesting a causal link between the movement of the sand and the origin of the doming and wrinkling of the overlying laminae.

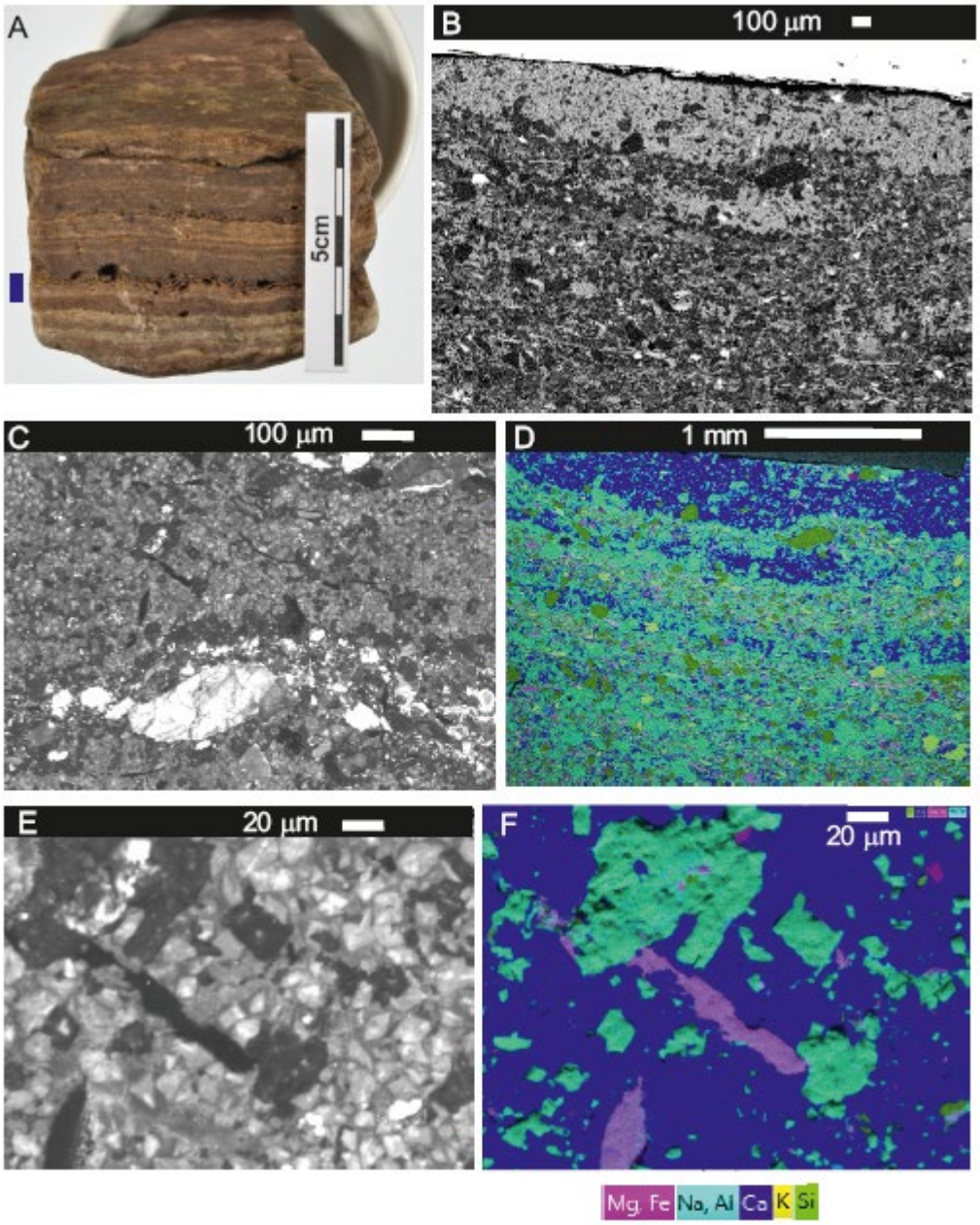

650

651 Fig. 5: Clachtoll flat-laminated sediments as seen in hand-specimen (A) and under the electron
652 microscope (B-F). B: a calcite lamina (top, light grey) as seen in backscatter, with silicate laminae
653 appearing darker in tone. C: cathodoluminescence (CL) image of the carbonate band shown in B
654 (scale bar is 100 microns). D: Energy Dispersive X-ray (EDS) element map showing Ca (calcite, blue),
655 Na, Al, Si areas (feldspars and aluminosilicates, blue-green), SiO phases (quartz, green) and Mg, Fe
656 silicates (micas, pink). E: higher magnification CL image of the calcite-rich area, showing grain
657 textures, with grains being predominantly euhedral to subhedral calcite crystals. F: EDS map of the
658 same area as seen in E, showing that the dark patches in E are silicates, and luminescing areas are
659 consistent with calcite.

660

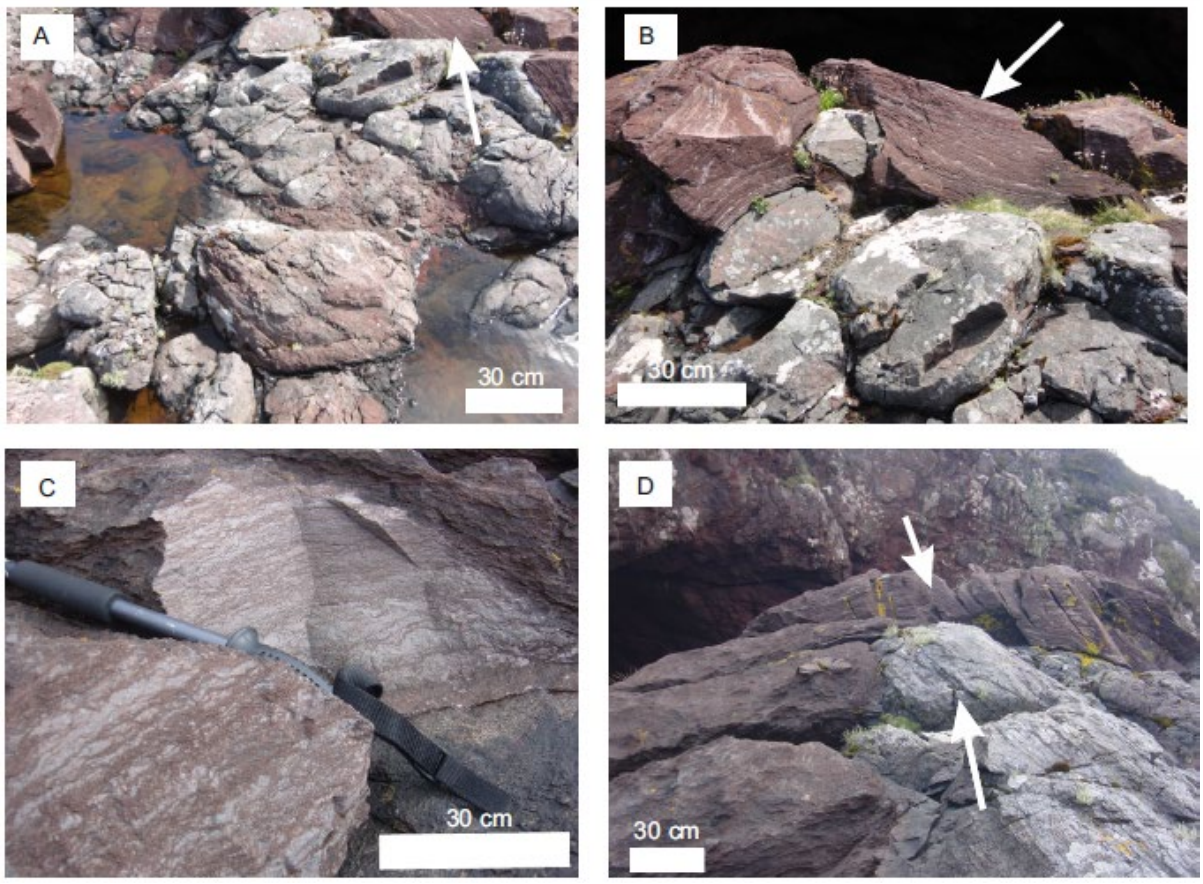

661

662 Fig. 6: Poll a' Mhuilt member at Enard Bay. A) Palaeo-land surface of Lewisian gneiss that had been
663 weathered into boulders and cobbles that were later draped over by the Poll a Mhuilt Member
664 possible stromatolites (arrowed) B) Possible stromatolites draping the surface (arrowed), C) Possible
665 stromatolites in cross-section are comprised of calcite (grey) and siliciclastic (red) laminae, D) a side
666 view showing the layer of possible stromatolitic sediment (short arrow) draping over the
667 Palaeoproterozoic gneiss boulders and cobbles (long arrow).

668

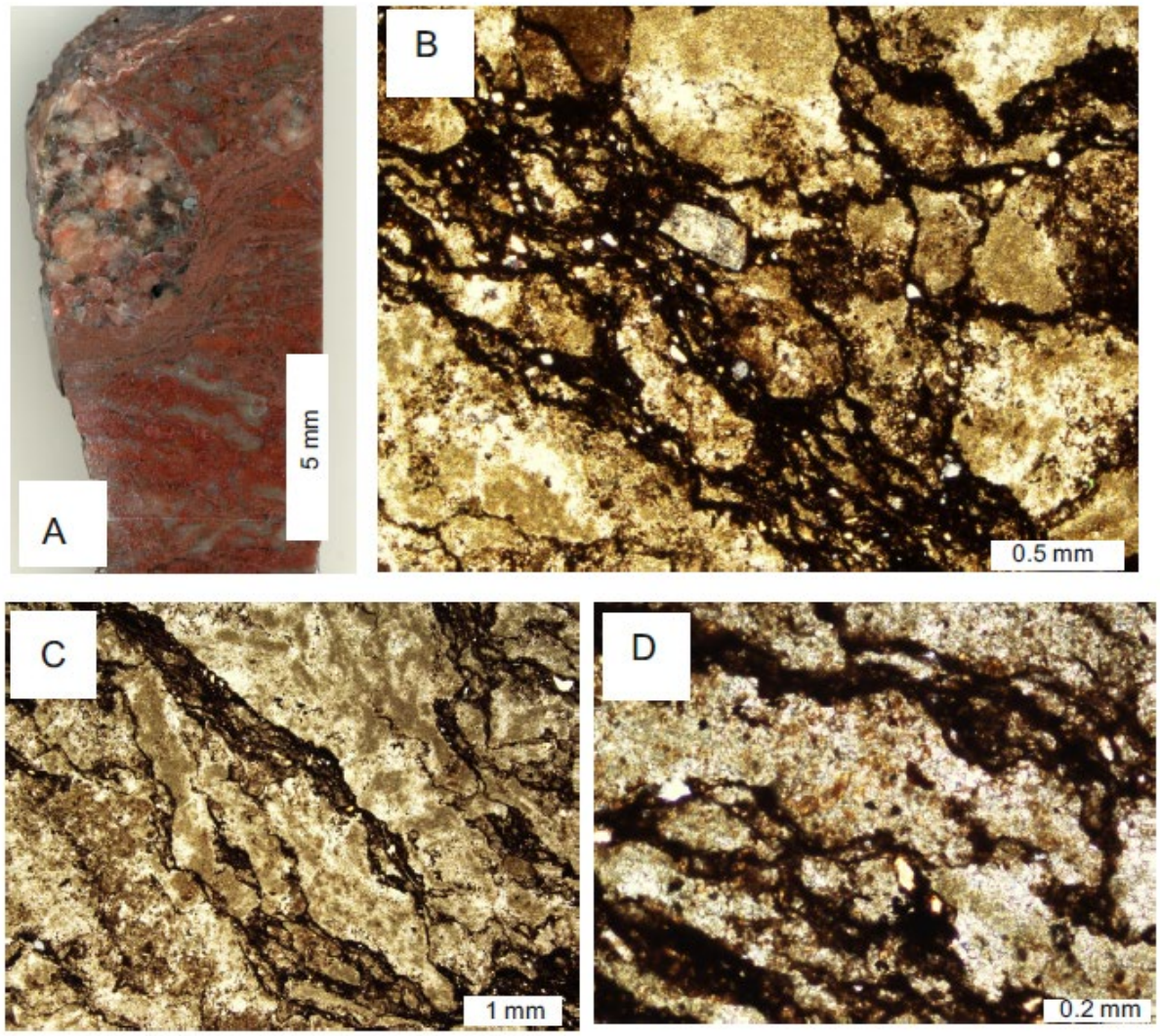

669

670 Fig. 7: optical petrography of possible stromatolite material from the Poll a'Mhuilt Member at Enard
671 Bay. A) stereomicroscope image of a cut hand-specimen, showing a gneiss clast (top left)
672 encapsulated in laminae of calcite (grey) and siliciclastic sediment (red). B) Thin-section of possible
673 stromatolite, showing clasts of calcite with some smaller clasts of feldspar and quartz within a dark
674 coloured matrix of siltstone. C) and D) are similar to B. Note that D shows some included orange
675 'blobs' in the calcite that proved to be silicate minerals rather than microfossils.

676

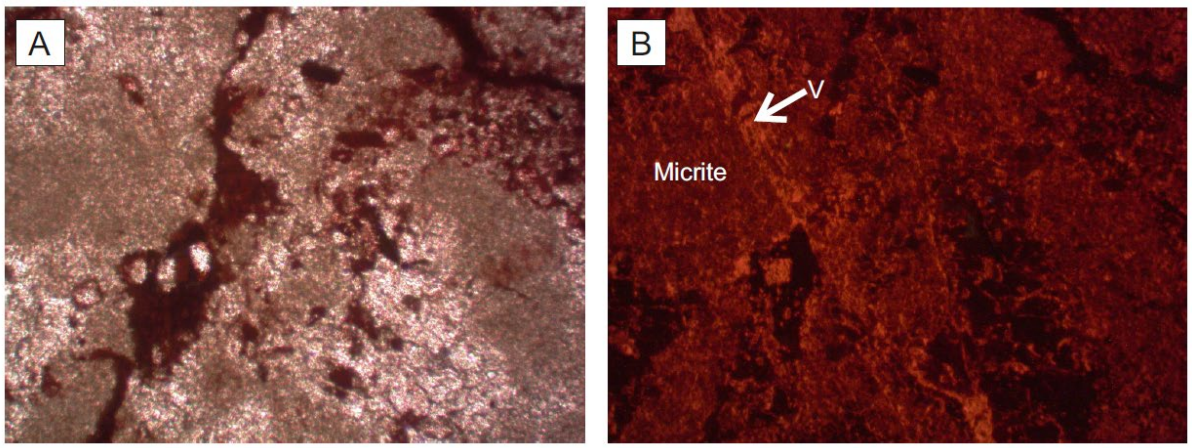

677

678 Fig. 8: cold cathode cathodoluminescence (CL) of possible stromatolite material from the Poll
679 a'Mhuilt Member at Enard Bay. A) plane polarised light, and B) CL image of the same area. Micrite is
680 orange-red luminescent, vein calcite (arrowed, V) is bright orange luminescent, and some patches of
681 spar (Sp) are non-luminescent.

682

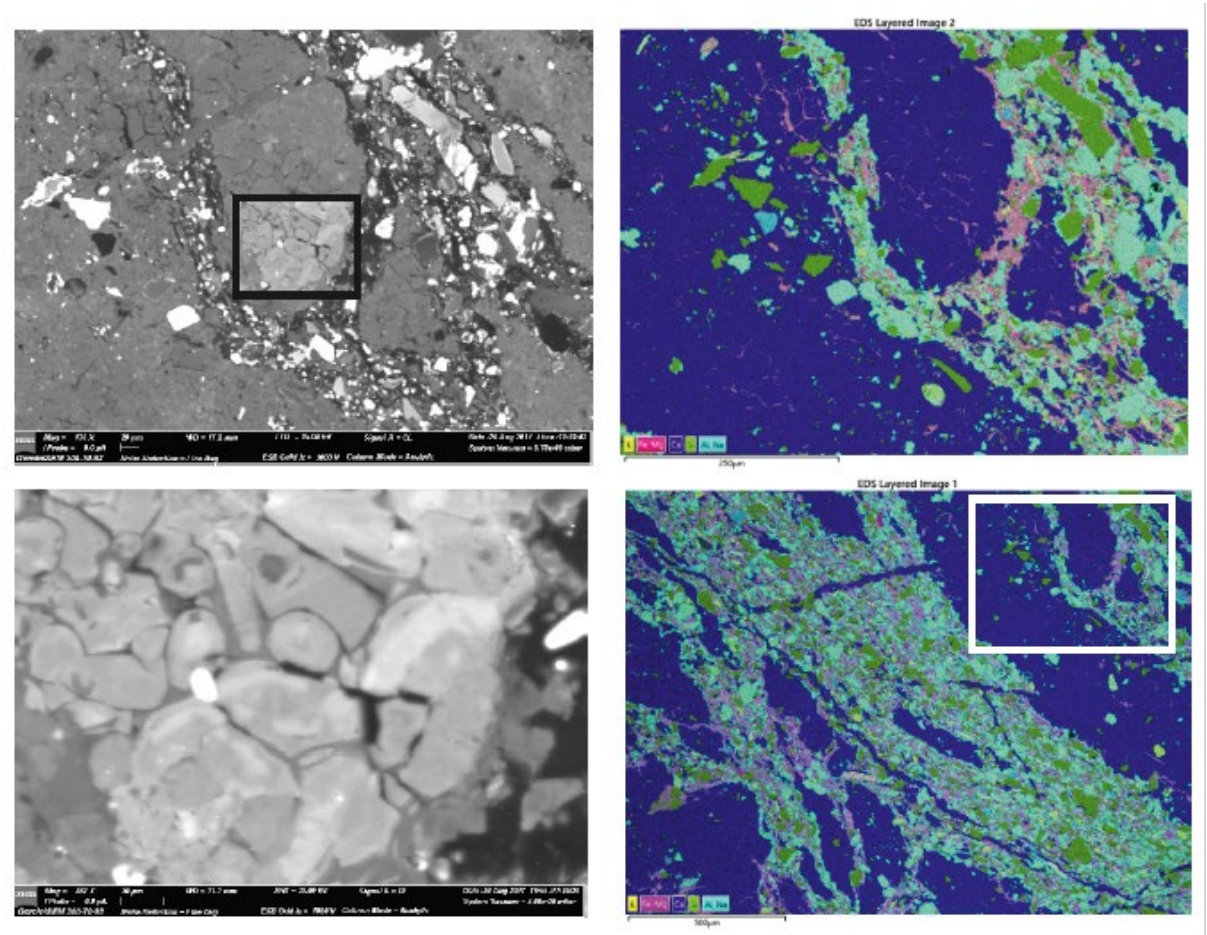

683

684 Fig. 9: Scanning Electron Microscope CL (top left and lower left) and EDS (top right and lower right)
685 images of stromatolite material from the Poll a'Mhuilt Member at Enard Bay. Top left and top right
686 show the same area. Lower right is at lower magnification giving context (white box shows are

shown in top images). Lower left is a close-up of the area within the black box in the top left image. The CL images show composite grains of calcite (Ca-rich areas, blue in EDS images) with patches of Fe-Mg rich aluminosilicates (pink in EDS images) between the component sub-grains. Between the composite grains are further aluminosilicates, Na-rich feldspars (light blue in EDS images) and quartz (green in EDS images).

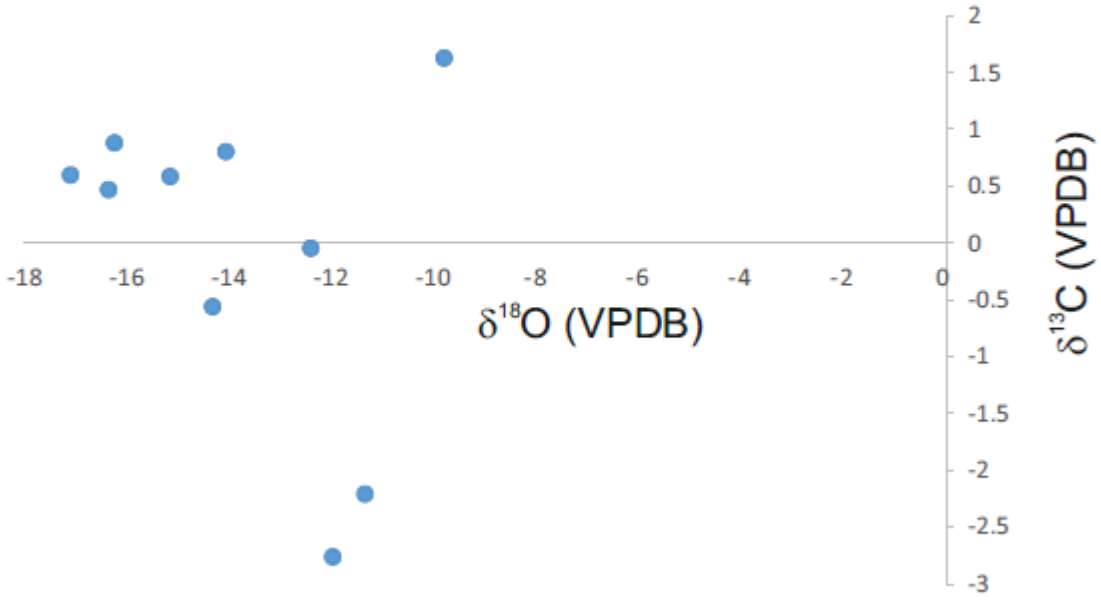

Fig. 10: Carbon ($\delta^{13}C$ vs VPDB) and oxygen ($\delta^{18}O$ vs VPDB) stable isotopes of Stoer Group carbonates. Data plotted are those given in Table 1.

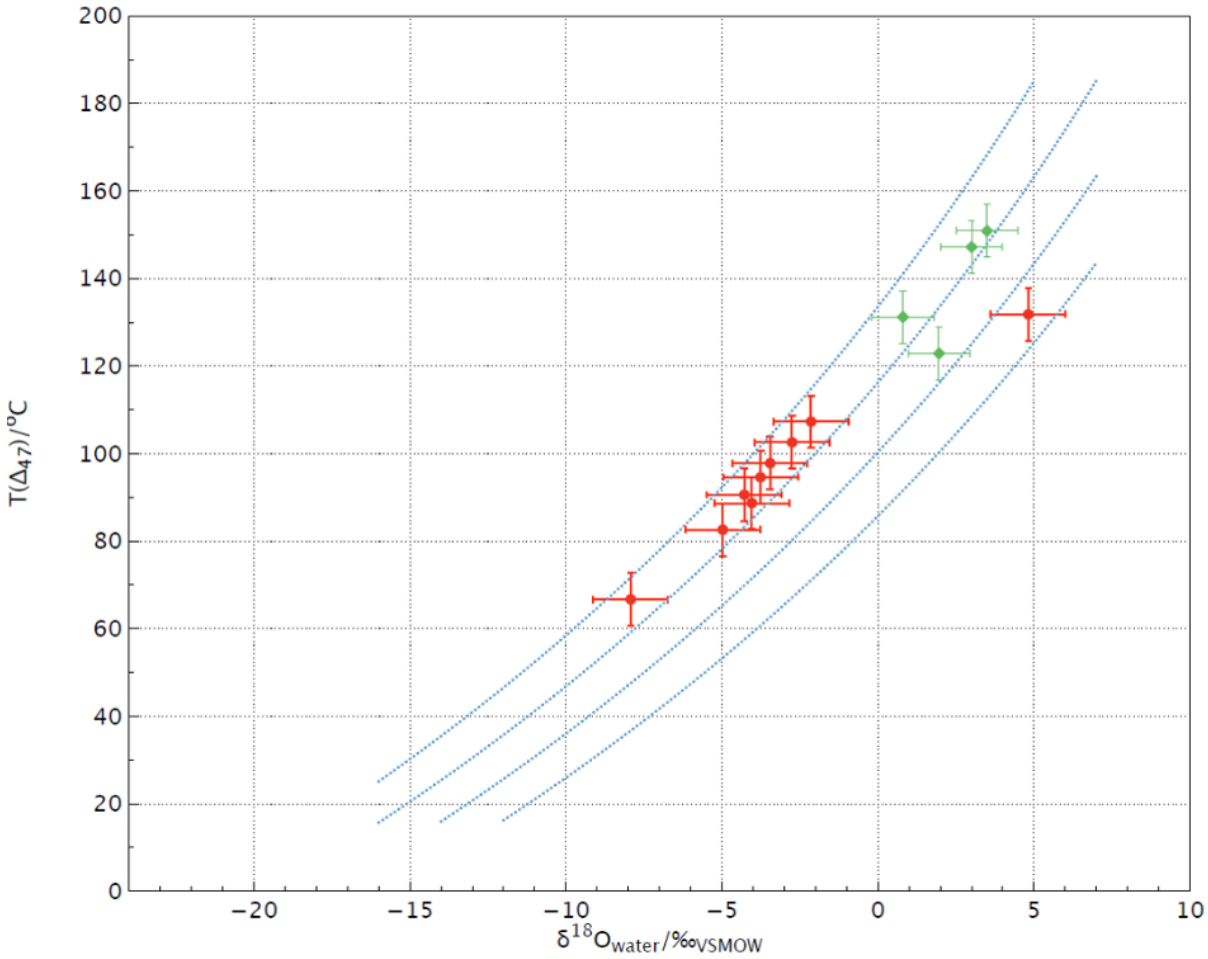

Fig. 11: Clumped isotope palaeothermometry of examined carbonate minerals. Calculated temperatures (T (Δ_{47}) in °C on the Y axis, and $\delta^{18}O_{water}$ (VSMOW) on the X axis. Calculated fluid compositions are those that would be in isotopic equilibrium with calcite at the notional temperature. Enard Bay Poll a'Mhulit member "stromatolitic" carbonates are plotted in green on the diagram. The red data set is from Bay of Stoer. The bulk of the Bay of Stoer data come from two thin limestone bands close to the top of the red shales of the Poll a' Muilt group, with some data from the 'tufted stromatolites' described by Upfold (1984).

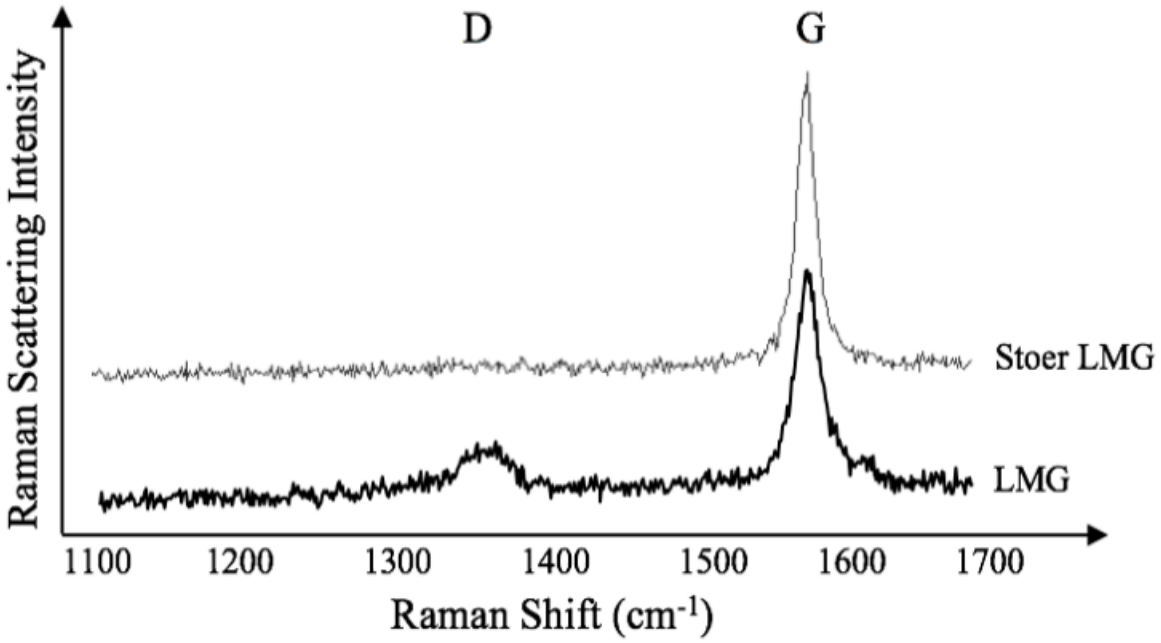

706

707 Fig. 12: Representative stacked first order Raman scans for Loch Maree Group (LMG) graphite
708 (modified after Muirhead *et al,* 2016) and the detrital LMG graphite within the Stoer Group (Stoer
709 LMG).

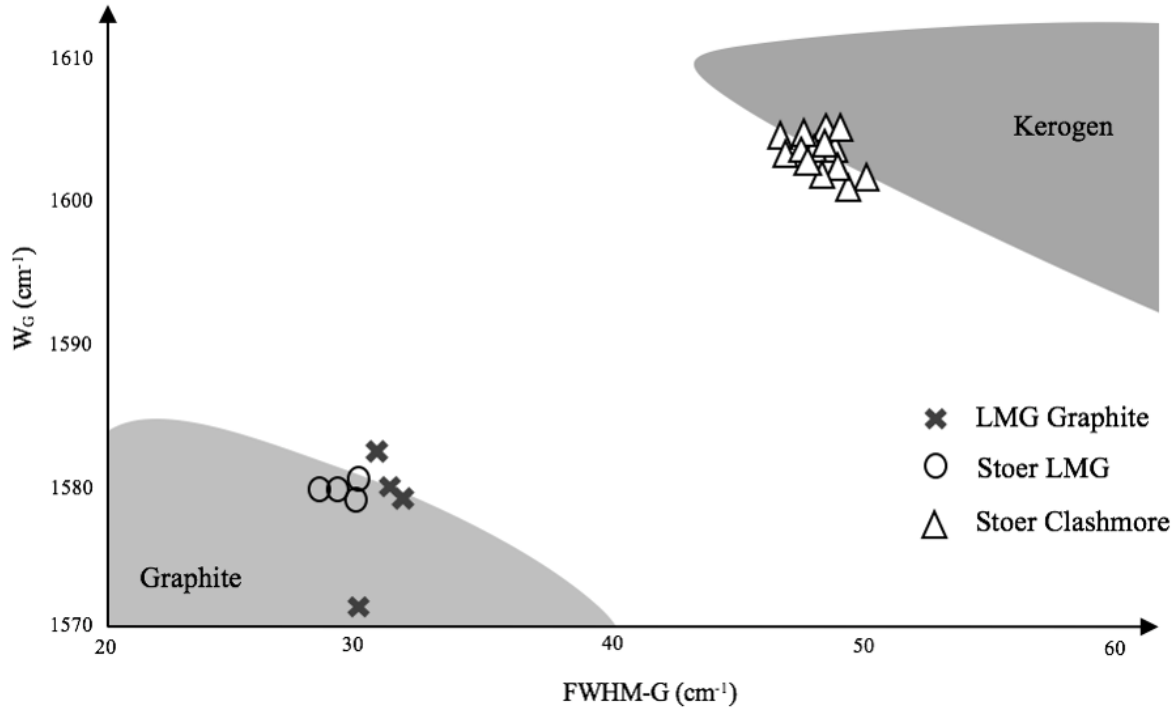

710

711 Fig. 13: Raman cross-plot of FWHM-G (cm^{-1}) and G band position (W_G, cm^{-1}) for the Loch Maree Group
712 (LMG) graphite (modified after Muirhead *et al,* 2016) and the detrital graphite within the Stoer Group
713 (Poll a' Mhuilt Member, Enard Bay). Stoer Group Clashmore plot adapted from Muirhead *et al,* 2016.